Nylon Fibers as Template for the Controlled Growth of Highly Oriented Single Crystalline ZnO Nanowires

ARTICLE *in* CRYSTAL GROWTH & DESIGN · MAY 2013

Impact Factor: 4.89 · DOI: 10.1021/cg400483d

2 AUTHORS:

Thushara Athauda
Oklahoma State University - Stillwater
19 PUBLICATIONS **142** CITATIONS

SEE PROFILE

Ruya R Ozer
Radford University
25 PUBLICATIONS **301** CITATIONS

SEE PROFILE

CRYSTAL GROWTH & DESIGN

Article

pubs.acs.org/crystal

Nylon Fibers as Template for the Controlled Growth of Highly Oriented Single Crystalline ZnO Nanowires

Thushara J. Athauda and Ruya R. Ozer*

Department of Chemistry and Biochemistry, University of Tulsa, Tulsa, Oklahoma 74104, United States

Supporting Information

ABSTRACT: This article reports the first controlled synthesis of large scale continuous arrays of single-crystalline ZnO nanowires with tunable size and properties on nylon fibers using a two-step low-temperature hydrothermal growth strategy. This process involves seed treatment of the substrate with ZnO nanocrystals that will form nucleation sites for subsequent epitaxial growth of single crystalline ZnO nanowires. Well-defined, vertically oriented, highly dense, and uniform ZnO nanowires of the wurtzite crystal structure covering the entirety of the fibers were achieved. In order to study the size and shape-dependent optical and electrochemical properties of the nanowires, the seed-to-growth solution concentration ratio was varied, resulting in hexagonal flat-ended (nanorods) and tapered (nanoneedles) morphologies. The amount of ZnO nanorods and nanoneedles grown on nylon fibers were determined as 30.1 ± 0.5% and 11.4 ± 0.7% ZnO by weight, respectively. In comparison to nanorods, ZnO nanoneedles demonstrated enhanced crystallinity, better orientation along the *c*-axis, and widened band gap. A similar trend was observed in the UV−vis absorption of nanorods and nanoneedles, the absorption-edge of the latter exhibiting a blue-shift that correlates with the widening of the band gap with nanoneedle formation. Moreover, the surface charge transport properties showed strong dependence on the ZnO morphology in which ZnO nanorods exhibited lower surface charge transfer resistance.

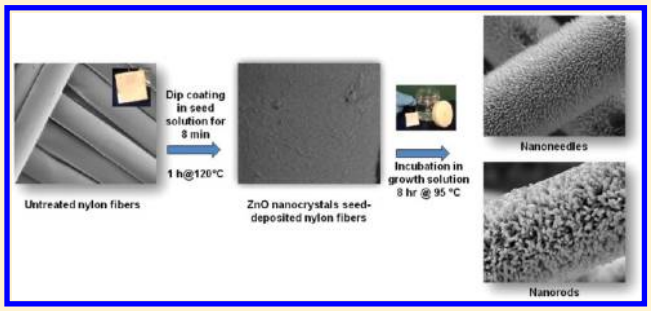

1. INTRODUCTION

Growing uniform, highly oriented, single-crystalline, and continuous arrays of metal-oxide semiconductor nanowires on flexible substrates such as plastic, paper, and textiles is of significant importance for the development of wearable electronics, smart clothing with sensing and protection capabilities, and portable and flexible photovoltaic devices.[1−4] Among various compound semiconductors, ZnO has been one of the most extensively studied for the generation of conductive electrodes,[5] solar cells,[6−11] gas sensors,[12,13] photosensors,[14,15] and piezoelectric devices.[16−19] ZnO also has a potential application in photocatalytic degradation of hazardous compounds with UV illumination.[20−22] As a result of its relatively large band gap (3.37 eV), it has been grown on a wide range of surfaces for generating protection against UV radiation as well as water and oil repellency.[23−32] Versatility of applications requires a precise control over the structure (size, shape, orientation, and crystallinity) since the structure determines the physical, chemical, and optical properties of the desired functional materials and devices.[33,34] For example, Baruah et al. have shown that ZnO nanorods have a higher photocatalytic activity compared to that of thin films due to their enhanced surface area-to-volume ratio.[20] In addition, well oriented thin and continuous arrays of nanorods were found to shorten the electron transport pathways and promote the separation of charge carriers.[35,36]

ZnO nanowires have been generally synthesized by chemical or physical vapor deposition.[37] Yet, they require high temperatures (350 ≥ °C) and sophisticated equipments. An alternative solution-based technique,[38−45] more environmentally friendly, economical, and straightforward, has been developed and preferred for the growth of monodisperse, well-aligned, single crystalline, and high aspect ratio ZnO nanowires, especially on temperature-sensitive surfaces such as fibers[27,29,30,46−49] and paper.[50−52] The hydrothermal growth method typically follows a two-step route, which involves a seeding step of a surface and a subsequent solution deposition process, resulting in epitaxial crystal growth of ZnO nanowires. As a result of the intrinsic anisotropy in the growth rate, predominantly hexagonal ZnO nanorods of wurtzite structure have been synthesized and studied. Size, shape, and the degree of crystallinity can be modulated by the synthesis parameters such as the precursor concentrations, temperature, and the duration of the synthesis.[34,53,54] For instance, Cheng and Samulski reported that the change in precursor concentrations resulted in nanorods with distinct aspect ratios.[55] The high aspect ratio ZnO nanowires had a higher degree of crystallinity and widened band gap compared to their low aspect ratio hexagonal counterparts. Therefore, a quantitative roadmap of

Received: April 2, 2013
Revised: May 2, 2013
Published: May 9, 2013

dx.doi.org/10.1021/cg400483d | *Cryst. Growth Des.* 2013, 13, 2680−2686

the structure−property relationship for the controlled growth of surface-bound ZnO nanowires is required for further application of these materials in future nanodevices.

In this work, we report for the first time controlled synthesis of large scale continuous arrays of single crystalline ZnO nanowires with tunable morphology and optical and electrochemical properties on nylon fibers using an optimized two-step low-temperature hydrothermal growth strategy. Well-defined, vertically oriented, highly dense, and uniform ZnO nanowires with wurtzite crystal structure were obtained that covered the entirety of the fibers as depicted in Figure 1. ZnO

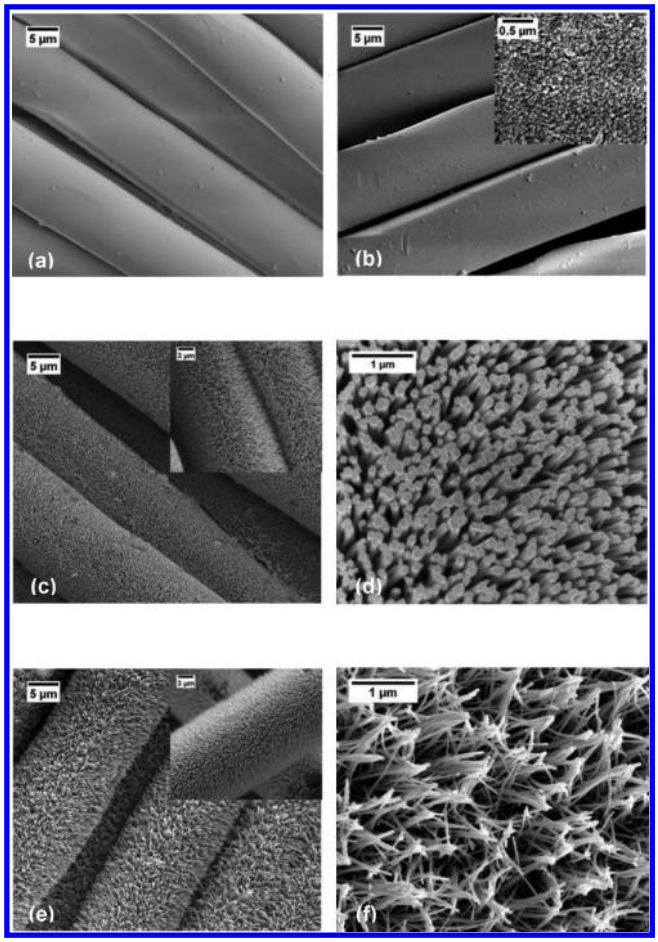

Figure 1. SEM images of (a) unmodified nylon fibers, (b) ZnO seed deposited nylon fibers (inset: high magnification images), (c,d) high and low magnification of ZnO nanorods grown on nylon fibers, and (e,f) high and low magnification of ZnO nanoneedles grown on nylon fibers.

nanowires were found to exhibit preferential growth orientation along the *c*-axis. The controlled synthesis of ZnO nanowires was based on the seed treatment of nylon fibers with ZnO nanocrystals that form nucleation sites for subsequent homoepitaxial growth of single crystal ZnO nanowires. Briefly, ZnO nanocrystals were first deposited on nylon swatches (2 cm × 2 cm) by dip-coating in a 100 mM solution of zinc acetate dihydrate in isopropyl alcohol with equimolar amount of triethylamine. After a short incubation (8 min), the swatches were removed from the seed solution, cured at 120 °C for 1 h, and then dried thoroughly in air. These ZnO seed-deposited nylon samples were split into two batches to study the effect of the seed-to-growth solution concentration ratio ([S]/[G]) on the structure (size, shape, orientation, and crystallinity) of the ZnO nanowires and concomitant optical and electrochemical properties. To ensure uniform growth of the ZnO nanowires, nylon fabric was immobilized on individual glass coverslips using an epoxy glue and then suspended vertically in ZnO growth solutions each composed of zinc nitrate hexahydrate (25 mM and 100 mM) and equimolar amounts of hexamethylenetetramine. Therefore, two samples with [S]/[G] of 1.0 and 4.0 were obtained. After incubating in the growth solutions for 8 h at 95 °C, the swatches were washed with deionized water, air-dried, and then evaluated. All characterizations and measurements were carried out with the modified and control samples attached to the glass coverslips. The optimized two-step hydrothermal process for growing ZnO nanowires on nylon fibers is illustrated in Scheme 1.

It is worthwhile to mention that a study concerning the growth of ZnO nanorods on nylon fabric has previously been reported by Xue et al.[56] This study was limited to a single [S]/[G] value and lacked extensive analysis of the structural dependence of physical, optical, and electrochemical properties of ZnO nanorods. Moreover, the optimized hydrothermal growth strategy reported in our work yielded modified fibers with 30.1 ± 0.5% ZnO by weight compared to that of only 14 wt % reported in the aforementioned study.

2. EXPERIMENTAL SECTION

2.1. Materials. The nylon fabric was purchased from TestFabrics (West Pittson, PA). Zinc acetate dihydrate ($Zn(CH_3COO)_2{\cdot}2H_2O$, ACS reagent, ≥ 98%), triethylamine ($(C_2H_5)_3N$ ≥ 99.5%), isopropyl alcohol (C_3H_8O, anhydrous, 99.5%), sodium hydroxide (NaOH, ACS reagent, ≥97.0%, pellets), citric acid ($C_6H_8O_7$, ACS reagent, ≥99.5%), Triton X-100 (laboratory grade nonionic surfactant), zinc nitrate hexahydrate ($Zn(NO_3)_2{\cdot}6H_2O$, reagent grade 98%), and hexamethylenetetramine ($C_6H_{12}N_4$, ACS reagent, ≥99.0%) were purchased from Sigma-Aldrich.

2.2. Scouring of Nylon Fabric. Before ZnO nanowires were grown, nylon fabric was cut into square swatches (2 cm × 2 cm) and scoured to remove wax, grease, and other finishing chemicals. The scouring solution was prepared by first dissolving 5.0 g of NaOH in 20 mL of deionized water followed by the addition of 1.5 g of Triton X-100 and 0.75 g of citric acid. The resulting solution was then diluted to 500 mL with deionized water. In the scouring process, four nylon swatches were then placed in a 500 mL round-bottom flask containing 200 mL of the scouring solution. The mixture was then stirred at 100 °C for 1 h. The scoured swatches were removed from the solution, rinsed thoroughly with DI water, and dried in air.

2.3. Preparation of ZnO Seed Solution. ZnO seed solution was prepared as follows. First, a 100 mM solution of zinc acetate dihydrate was prepared by dissolving 1.10 g (5.0 mmol) in 50.0 mL of isopropyl alcohol. The resulting solution was then stirred vigorously at 85 °C for 15 min. After this time, 700 μL of triethylamine (5.0 mmol) was added dropwise to the stirred solution. The resulting solution, now clear, was stirred at 85 °C for an additional 10 min. After this time, the solution was cooled to room temperature and incubated without stirring for 3 h. The pH of the seed solution was 7.01 (pH meter). The average particle size of the ZnO nanocrystal seed solution was 31.5 ± 10.0 nm, as measured by a Zetatrack (Microtrac) particle size analyzer. We have used this seed solution up to 2 weeks after its preparation with no discernible change in the final ZnO nanocrystals.

2.4. Preparation of ZnO Growth Solution. Equimolar aqueous solutions of zinc nitrate hexahydrate and hexamethylenetetramine were used to grow ZnO nanorods on nylon swatches. First, a 100 mM solution of hexamethylenetetramine was prepared by dissolving 7.71 g (5.0 mmol) in 550 mL of DI water. Once dissolved, 16.4 g of zinc nitrate hexahydrate (5.0 mmol) was added, and the resulting solution was stirred for 24 h at room temperature. The final pH of this ZnO growth solution was 6.11 (pH meter). A 50.0 mM solution of the ZnO

dx.doi.org/10.1021/cg400483d | *Cryst. Growth Des.* 2013, 13, 2680−2686

Scheme 1. Schematics of the Two-Step Hydrothermal Process for Growing ZnO Nanowires on Nylon Fibers

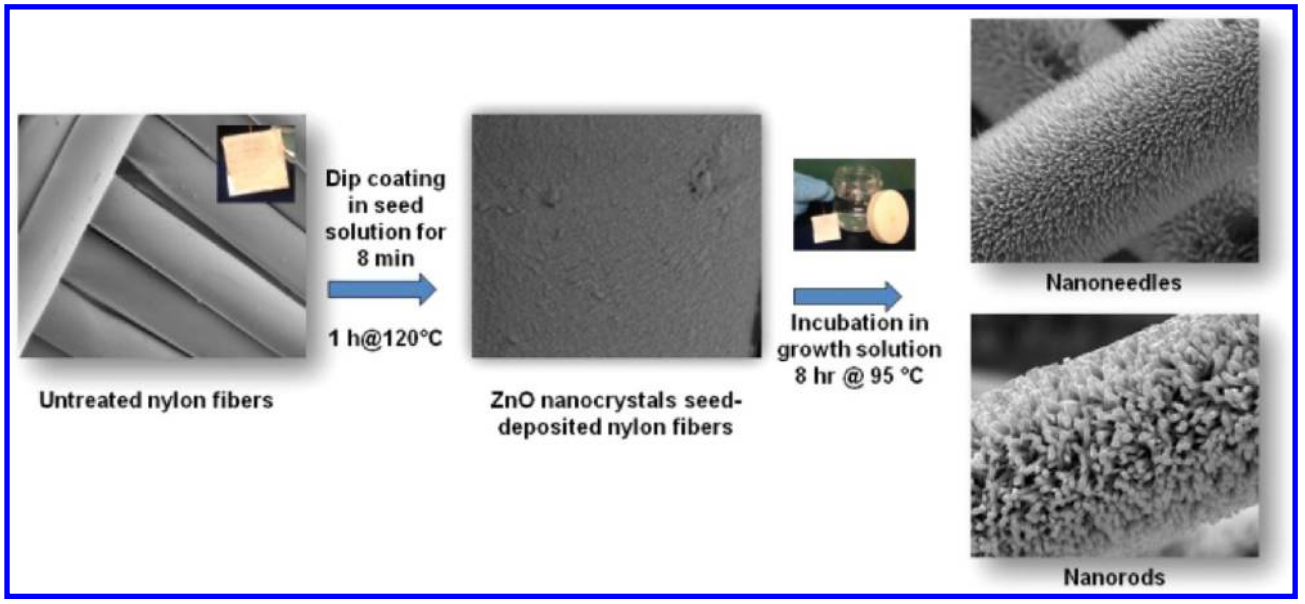

growth solution was also prepared by diluting 100 mM stock solution for the investigation of the effect of the seed-to-growth solution concentration ratio on the structural, optical, and electrochemical properties of the ZnO nanowires grown on nylon fibers.

2.5. Growth of ZnO Nanowires on Nylon Swatches. The scoured nylon swatches were first dip-coated with the ZnO seed solution for 8 min and then rinsed with ethanol. The dip-coated swatches were then suspended from a wire rack, cured at 120 °C for 1 h in an oven, and then further conditioned in air for 12 h at room temperature. To ensure uniform deposition of ZnO nanowires on nylon surfaces in subsequent steps, the swatches were then immobilized on a glass coverslip using an epoxy glue (LOCTITE stik'n seal ultra, Flextec Technology). The immobilized swatches were then suspended vertically in ~70 mL of the growth solution and incubated at 95 °C for 8 h in an oven. The container was removed from the oven, cooled to room temperature, and then further incubated at room temperature for 10–12 h. Finally, the swatches were removed from the growth solution, thoroughly rinsed with DI water, and allowed to air-dry at room temperature.

2.6. Characterization. Size, shape, and orientation of the ZnO nanowires grown on nylon fibers were investigated using a JEOL JSM 6060 LV field emission scanning electron microscope (FESEM). The samples were coated with a 5–10 nm Au layer before the SEM imaging. Elemental analyses of the samples were performed on the SEM system equipped with an EDAX TEAM operating at an accelerating voltage of 20 kV. Crystal structures were analyzed using a Shimadzu XRD-6100 X-ray diffractometer with Cu Kα radiation, employing a scanning rate of 0.02°/s within the range of 2θ =10–70°, operating at 40 kV and 33 mA (1320 W). Thermogravimetric analyses (TGA) were carried out using a Mettler Toledo 851 with a TSO 801RO robotic arm. The samples were heated from 40 to 600 °C at a rate of 10 °C/min under a nitrogen atmosphere at a flow rate of 40 mL/min. UV-transmittance of the samples was studied using a Varian Cary 50 UV–vis spectrophotometer in the wavelength range of 280–480 nm and a scan rate of 300 nm/min. Photoluminescence (PL) studies were performed at room temperature using a dual-scanning microplate Jasco FP-6500 spectrofluorometer (version 1.08.02) with the Spectra Manager Software using the excitation wavelength at 325 nm. Electrochemical impedance measurements were performed with a computer controlled dielectric interface (Solartron 1296) equipped with an impedance/gain phase analyzer (Solatron SI 1260) in a sweep frequency range of 0.1–10^7 Hz.

3. RESULTS AND DISCUSSION

Figure 1 presents SEM images of unmodified, ZnO seed deposited, ZnO nanorods ([S]/[G] = 1.0), and ZnO nanoneedles ([S]/[G] = 4.0) grown nylon fibers. We define nanorods as the structures with well-defined facets and hexagonal cross sections and clear-cut flat ends. Nanoneedles, however, have tapered tips and rounded cross sections with higher aspect ratios. Scoured nylon fibers have smooth surfaces with calculated average diameters of 11.7 ± 0.7 μm. After the seed treatment, ZnO nanocrystals formed discrete nucleation sites uniformly distributed over the entire fiber surfaces. The nucleation step is crucial for the epitaxial growth of ZnO nanowires.[57] Vertically aligned, uniform, and densely packed arrays of hexagonal ZnO nanorods were successfully achieved over the entire nylon fibers (Figure 1c,d) with an average diameter of 160 ± 12 nm and an approximate length of 1.76 ± 0.12 μm (aspect ratio = 11:1). Figure 1e,f depicts formation of ZnO nanoneedles when the [S]/[G] value was adjusted to 4.0. The average length of the nanoneedles was 1.68 ± 0.12 μm with a diameter of 54 ± 10 nm (aspect ratio = 31:1). Figure 2

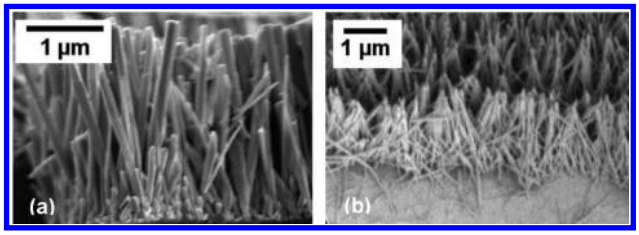

Figure 2. High magnification cross-sectional SEM images of (a) ZnO nanorods grown on nylon fibers and (b) ZnO nanoneedles grown on nylon fibers.

reveals high magnification cross-sectional SEM images of ZnO nanorods and nanoneedles that were obtained using two distinct [S]/[G] values. Although the length of the ZnO nanorods and nanoneedles are similar, the aspect ratios differ drastically, which also results in significant variations in optical and electrochemical properties. Our observation is in agreement with Vayssieres' report that the decrease in concentration

dx.doi.org/10.1021/cg400483d | Cryst. Growth Des. 2013, 13, 2680–2686

of the precursors would result in a drop in the diameters of the ZnO nanorods.[43]

The cluster morphology observed in Figure 2 is fairly common and suggests that multiple nanorods frequently grow from a single aggregate of the ZnO nanocrystal seeds deposited onto the nylon fibers. Even though the ZnO morphology evolved from rod- to needle-like structures, single crystallinity of the wurtzite family was maintained, as indicated in the XRD results (Figure 4). Formation of the sharp-tipped nanoneedles might be due to the gradual depletion of the growth solution, which could yield a concentration gradient of Zn from the base to the tip. These results correlate well with previous reports suggesting that the shape of the ZnO nanostructures are very sensitive to the overall concentration of the precursors, in which the particle diameters became smaller with decreasing concentrations.[33,39]

Chemical composition of the ZnO nanowires grown on nylon fibers was verified by energy dispersive X-ray (EDX) spectroscopy. Figure 3a–d displays EDX micrographs of an unmodified, ZnO seed deposited, ZnO nanoneedles, and ZnO nanorods grown nylon fibers. The nylon fibers do not contain any contaminants, indicated by the sole presence of carbon (C) and oxygen (O) atoms. Figure 3b–d reveals that the ZnO modified nylon sample contains only zinc (Zn), carbon, and oxygen atoms, indicating high purity of the grown ZnO nanorods and nanoneedles.

The degree of crystallinity of the ZnO nanowires was determined by X-ray diffraction spectroscopy. Figure 4 shows XRD patterns of unmodified, ZnO nanoneedles, and ZnO nanorods grown nylon fibers. The peaks at 2θ values of 17.5°, 23.0°, and 26.5° that were observed for the unmodified nylon fibers correspond to crystalline domains of polyamides.[58] Six reflection peaks appeared at 2θ values of 31.9° (100), 34.6° (002), 36.5° (101), 47.7° (102), 56.8° (110), and 63.1° (103) for the ZnO nanowires can be indexed as the hexagonal wurtzite structure. The narrow full width at half-maximum (fwhm) of the ZnO peaks shows that ZnO nanowires are well crystallized. Anisotropic growth was shown to be a common characteristics of the wurtzite structure. No diffraction peaks from any other impurity phases are found, confirming that the only single-phase hexagonal ZnO is present. The (002) diffraction peak is significantly enhanced for the ZnO nanowires, indicating preferential growth along the *c*-axis for both morphologies. In many previous works, calcination at higher temperatures (≥300 °C) has been required to achieve single crystal ZnO nanostructures. However, we achieved a high degree of crystallinity, using relatively low-temperature hydrothermal growth technique on a flexible surface notoriously difficult to work with, that is comparable in terms of quality to that obtained using high-temperature methods and/or calcination.

Compositional ZnO content of the modified nylon fibers was further assessed by thermogravimetric analysis (TGA). Figure 5 presents the thermograms of the unmodified, seed layer deposited, and ZnO nanorod, and ZnO nanoneedles grown nylon samples. The amount of ZnO deposited on the nylon fibers after the seeding and the growth step was calculated by the weight loss of the samples at the end of the heating cycle. The nylon fibers deposited with the ZnO seed layer contained 2.5 ± 1.0% ZnO by weight, while the nylon bearing ZnO nanorods and nanoneedles contained 30.1 ± 0.5% and 11.4 ± 0.7% ZnO by weight, respectively. The weight of all samples was observed to drop sharply between 350 and 460 °C, and the total decomposition of the unmodified nylon is completed around 600 °C. Although there was no significant delay on the onset of the thermal decomposition of the nylon fibers, the rate of decomposition was considerably slowed, which can be attributed to the presence of the ZnO nanowires.

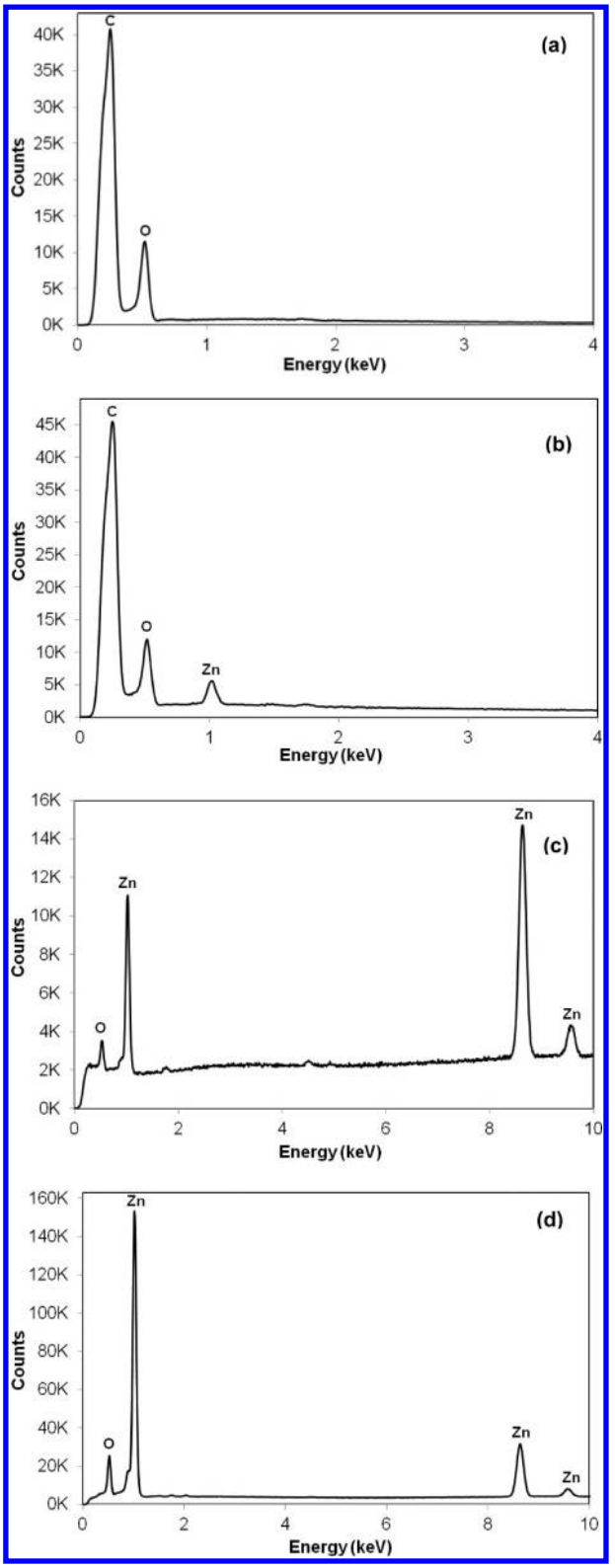

Figure 3. EDX analysis of (a) unmodified nylon fibers, (b) ZnO seed deposited, (c) ZnO nanoneedles grown, and (d) ZnO nanorods grown nylon fibers.

dx.doi.org/10.1021/cg400483d | *Cryst. Growth Des.* 2013, 13, 2680–2686

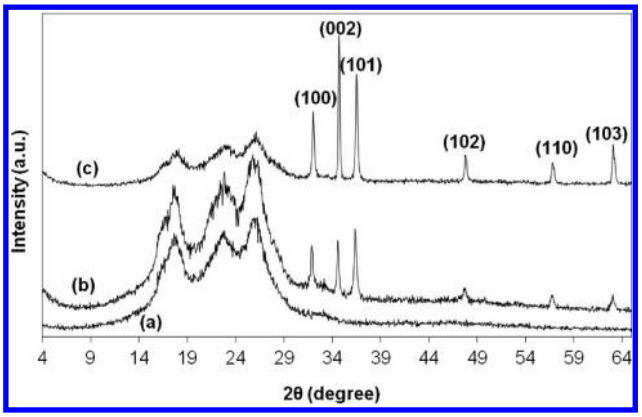

Figure 4. Indexed XRD patterns of (a) unmodified nylon fibers, (b) ZnO nanoneedles grown, and (c) ZnO nanorods grown nylon fibers.

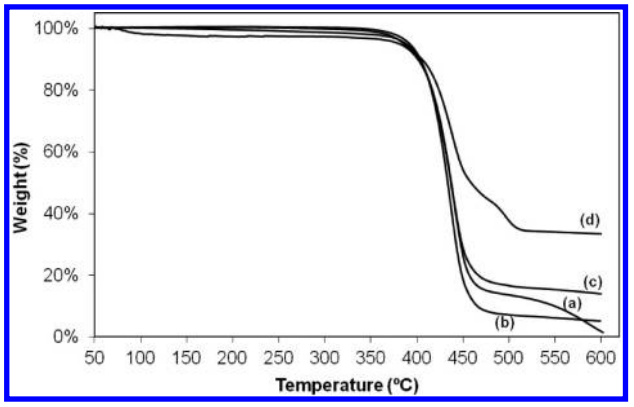

Figure 5. Thermograms of (a) unmodified nylon fibers, (b) ZnO seed deposited, (c) ZnO nanoneedles grown, and (d) ZnO nanorods grown nylon fibers.

To examine the structural dependence of the optical properties of ZnO nanowires, room-temperature photoluminescence spectra (PL) induced by 325 nm excitation wavelength were collected over a range of 350−600 nm. The spectra in Figure 6 are characteristics of an n-type ZnO semiconductor (E_g = 3.37 eV) with a near band-edge emission of 387 nm that is due to the recombination of excitons and a visible deep-level emission of 470 nm that is attributed to the structural defects. In general, the PL spectrum of powder or polycrystalline thin film shows much stronger visible emissions

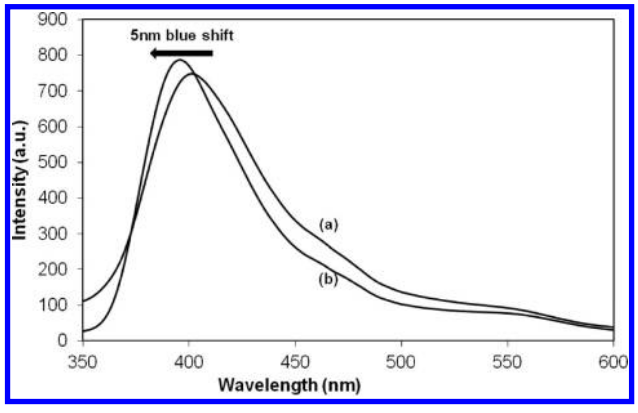

Figure 6. Photoluminescence spectra of (a) ZnO nanorods grown nylon fibers and (b) ZnO nanoneedles grown nylon fibers.

than UV emissions, while the epitaxial thin films on lattice-matched single-crystalline substrates show weaker visible emissions because of the reduced structural defects, as is the case in this study. ZnO nanorods and nanoneedles all have significantly lower visible emissions compared to the UV emissions, confirming the high crystallinity of the grown nanowires. The UV absorption edge of ZnO nanoneedles shifts toward blue about 5 nm compared to nanorods, indicating the widening of the band gap with nanoneedles formation. The observed morphology-dependent shift in the peak positions of the band-edge recombination might be due to the different native defect concentrations originating from surface/volume ratio differences.[59] Our observation corroborates well with the previous report showing a band gap increase with the reduced size for colloidal solutions by Greene et al.[40]

Optical properties of surface-bound ZnO nanowires were further assessed by UV−vis transmission spectroscopy. ZnO strongly absorbs in the UV region. Figure 7 depicts the

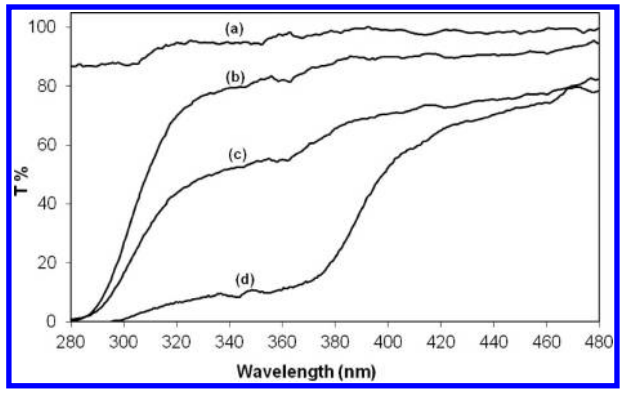

Figure 7. UV-transmission spectra of (a) unmodified nylon, (b) ZnO seed deposited, (c) ZnO nanoneedles grown, and (d) ZnO nanorods grown nylon fibers.

transmittance spectra of unmodified nylon, ZnO seed deposited, ZnO nanoneedles, and ZnO nanorods grown nylon fibers over the wavelength range of 280−480 nm. Untreated nylon absorbs only 18% of the radiation over the entire region. The presence of nanorods and nanoneedles significantly increases the absorption and scattering of the radiation, nanorods being more effective than nanoneedles, which is not surprising since the amount of ZnO arrays that can absorb the incoming photons is much higher (30.1 ± 0.5 wt %) compared to that of nanoneedles (11.4 ± 0.7 wt %). ZnO nanorods start to absorb at 378 nm, while the absorption edge shifts toward blue at 335 nm with nanoneedle formation. UV−vis spectra of nanoneedles exhibiting a blue shift of the absorption onset provides further indication of the widening band gap with the nanoneedle formation, in agreement with the PL observations. These results suggest that the degree of crystallinity is significantly improved with the nanoneedle formation.

The AC impedance technique measures the resistance of the surface to a current flow when a voltage is applied. The results are presented in complex impedance plane plots (also known as Nyquist plots), in which the real part is plotted against the imaginary part of the impedance. The distinctive semicircle in the high frequency region represents the interfacial resistance of the material to electron transfer. The electron transfer resistance (R_{CT}) is equal to the diameter of the semicircle, which controls the electron-transfer kinetics. Figure 8 presents

dx.doi.org/10.1021/cg400483d | Cryst. Growth Des. 2013, 13, 2680−2686

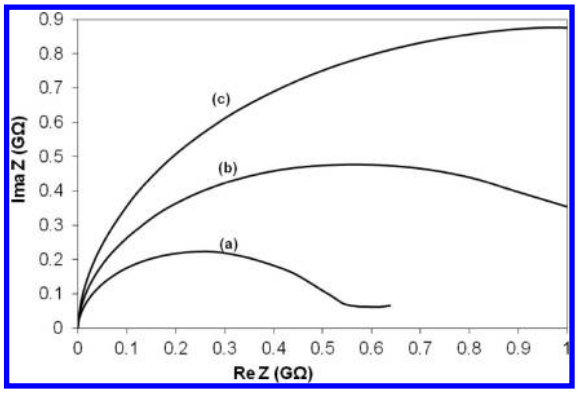

Figure 8. Electrochemical Impedance spectra of (a) ZnO nanoneedles grown nylon fibers, (b) ZnO seed modified, and (c) unmodified nylon fibers.

the impedance spectra of unmodified, seed deposited, and ZnO nanoneedles grown nylon fibers. The seed deposition easily caused the impedance to decrease by half. With the nanoneedles formation, the surface resistance dropped by almost an order of magnitude. The biggest change was observed with the nanorods growth, with which 3 orders of magnitude drop was observed, as seen in Figure 9. These results may be a significant step toward the development of flexible wearable electronics utilizing oriented 1D ZnO nanowires.

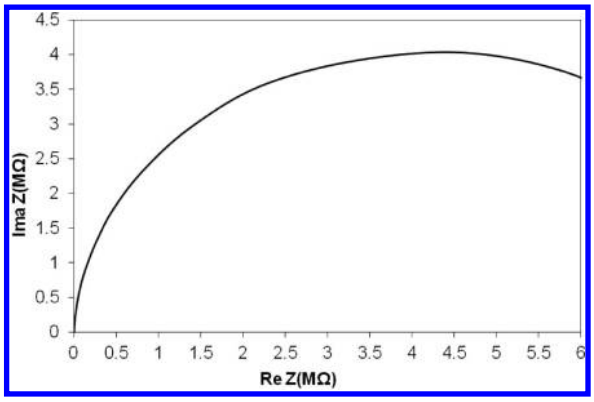

Figure 9. Electrochemical Impedance spectra of ZnO nanorods grown nylon fibers.

4. CONCLUSION

In this study, we have successfully grown ZnO nanorods and nanoneedles on nylon fibers by varying the seed-to-growth solution concentration ratio ([S]/[G]) in a two-step hydrothermal process. We have presented a systematic investigation on the most important synthesis parameter, seed-to-growth solution concentration ratio, affecting the structure of the ZnO nanowires grown on nylon fibers. We have observed that the [S]/[G] values determine the final morphology of the ZnO nanowires, which in turn affects the optical and electrochemical properties of the modified nylon surfaces. As a result, a quantitative roadmap for guiding the synthesis of ZnO nanowires that will possess targeted density, crystallinity, photoluminescence, UV absorption, and conductivity was obtained. Given that the performance of nanomaterials depends on their size, shape, and orientation, a clear understanding of the quantitative correlation between the structure and property is highly important for the development of nanostructured functional materials and devices. For instance, higher photoefficiency and surface conductivity are anticipated in view of the developed thin and continuous arrays of ZnO nanowires combined with directional mobility of charge carriers due to the quantum confinement effect. More importantly, ZnO nanoneedles with a high UV-absorption capacity, visible transparency, and widened band gap hold great promise for the development of wearable and/or flexible photovoltaics, transparent conductors, and protective clothing.

■ ASSOCIATED CONTENT

Supporting Information

Size distribution of the ZnO nanocrystals in the seed solution and images of the experimental setup. This material is available free of charge via the Internet at http://pubs.acs.org.

■ AUTHOR INFORMATION

Corresponding Author

*E-mail: ruya-ozer@utulsa.edu.

Notes

The authors declare no competing financial interest.

■ ACKNOWLEDGMENTS

We would like to thank The Department of Chemistry & Biochemistry at The University of Tulsa for its support. We greatly appreciate the financial support from The University of Tulsa Institute of Nanotechnology, TU Student Research Grants Program, and the Faculty Development Summer Fellowship and Research Programs for financial support. Paige Johnson, Rick Portman, Dr. Winton Cornell, and Dr. Parameswar Hari are acknowledged for technical assistance.

■ REFERENCES

(1) Lieber, C. M. *MRS Bull.* **2011**, *36*, 1052.
(2) Yang, P.; Wu, Y.; Yan, H.; Huang, M.; Messer, B.; Song, J. H.; Yang, P. *Chem.—Eur. J.* **2002**, 1260.
(3) Lee, M.; Kwak, G.; Yong, K. *ACS Appl. Mater. Interfaces* **2011**, *3*, 3350.
(4) Rogers, J. A.; Someya, T.; Huang, Y. *Science* **2010**, *327*, 1603.
(5) Scott, R. C.; Leedy, K. D.; Bayraktaroglu, B.; Look, D. C.; Zhang, Y. H. *Appl. Phys. Lett.* **2010**, *97*, 072113.
(6) Ravirajan, P.; Peiró, A. *J. Phys. Chem. B* **2006**, 7635.
(7) Thambidurai, M.; Muthukumaramsy, N.; Velauthapillai, D.; Arul, N.; Agilan, S.; Balasundaraprabhu, R. *J. Mater. Sci. Mater. Electron.* **2011**, *22*, 1662.
(8) Ko, S.; Lee, D.; Kang, H.; Nam, K.; Yeo, J. *Nano Lett.* **2011**, *11*, 666.
(9) Zhang, W.; Zhu, R.; Liu, X.; Liu, B.; Ramakrishna, S. *Appl. Phys. Lett.* **2012**, *043304*, 1.
(10) Mccune, M.; Zhang, W.; Deng, Y. *Nano Lett.* **2012**, *11*, 3656.
(11) Cheng, H.; Chiu, W.; Lee, C.; Tsai, S.; Hsieh, W. *J. Phys. Chem. C* **2008**, 1635.
(12) Wang, J. X.; Sun, X. Y.; Yang, Y.; Huang, H.; Lee, Y. C.; Tan, O. K.; Vayssieres, L. *Nanotechnology* **2006**, *17*, 4995.
(13) Spencer, M. J. S.; Yarovsky, I. *J. Phys. Chem. C* **2010**, *3*, 10881.
(14) Liu, J.; Wu, W.; Bai, S.; Qin, Y. *ACS Appl. Mater. Interfaces* **2011**, *3*, 4197.
(15) Su, Y. K.; Peng, S. M.; Ji, L. W.; Wu, C. Z.; Cheng, W. B.; Liu, C. H. *Langmuir* **2010**, *26*, 603.
(16) Bae, J.; Song, M. K.; Park, Y. J.; Kim, J. M.; Liu, M.; Wang, Z. L. *Angew. Chem., Int. Ed.* **2011**, *50*, 1683.
(17) Wang, Z. L. *MRS Bull.* **2012**, *37*, 814.
(18) Ahmad, M.; Zhu, J. *J. Mater. Chem.* **2010**, *21*, 599.
(19) Qin, Y.; Wang, X.; Wang, Z. *Nature* **2008**, *451*, 809.

(20) Baruah, S.; Mahmood, M. A.; Myint, M. T. Z.; Bora, T.; Dutta, J. *Beilstein J. Nanotechnol.* **2010**, *1*, 14.
(21) Baruah, S.; Jaisai, M. *Sci. Technol. Adv. Mater.* **2010**, 055002.
(22) Sugunan, A.; Guduru, V. K.; Uheida, A.; Toprak, M. S.; Muhammed, M. *J. Am. Ceram. Soc.* **2010**, *93*, 3740.
(23) Xu, B.; Cai, Z. *J. Appl. Polym. Sci.* **2008**, *108*, 3781.
(24) Qi, G.; Zhang, H.; Yuan, Z. *Appl. Sur. Sci* **2011**, *258*, 662.
(25) Xu, B.; Cai, Z.; Wang, W.; Ge, F. *Surf. Coat. Technol.* **2010**, *204*, 1556.
(26) Wang, L.; Zhang, X.; Li, B.; Sun, P.; Yang, J.; Xu, H.; Liu, Y. *ACS Appl. Mater. Interfaces* **2011**, *3*, 1277.
(27) Wang, R.; Xin, J.; Tao, X.; Daoud, W. *Chem. Phys.Lett.* **2004**, *398*, 250.
(28) Xu, B.; Cai, Z. *Appl. Surf. Sci.* **2008**, *254*, 5899.
(29) Preda, N.; Enculescu, M.; Zgura, I.; Socol, M.; Matei, E.; Vasilache, V.; Enculescu, I. *Mater. Chem. Phys.* **2013**, *138*, 253.
(30) Ates, E. S.; Unalan, H. E. *Thin Solid Films* **2012**, *520*, 4658−4661.
(31) Zhou, Z.; Zhao, Y.; Cai, Z. *Appl. Surf. Sci.* **2010**, *256*, 4724.
(32) Wang, L.; Zhang, X.; Fu, Y.; Li, B.; Liu, Y. *Langmuir* **2009**, *25*, 13619.
(33) Zheng, Y.; Chen, C.; Zhan, Y.; Lin, X.; Zheng, Q.; Wei, K.; Zhu, J.; Zhu, Y. *Inorg. Chem.* **2007**, *46*, 6675.
(34) Lee, Y. J.; Sounart, T. L.; Liu, J.; Spoerke, E. D.; McKenzie, B. B.; Hsu, J. W. P.; Voigt, J. A. *Cryst. Growth Des.* **2008**, *8*, 2036.
(35) Park, K.; Xi, J.; Zhang, Q.; Cao, G. *J. Phys. Chem. C* **2011**, *115*, 20992.
(36) Athauda, T. J.; Neff, J.; Sutherlin, L.; Ozer, R. R. *ACS Appl. Mater. Interfaces* **2012**, *4*, 6917.
(37) Bae, S. Y.; Seo, H. W.; Choi, H. C.; Park, J.; Park, J. *J. Phys. Chem. B* **2004**, *108*, 12318.
(38) Greene, L. E.; Law, M.; Goldberger, J.; Kim, F.; Johnson, J. C.; Zhang, Y.; Saykally, R. J.; Yang, P. *Angew. Chem., Int. Ed.* **2003**, *42*, 3031.
(39) Greene, L. E.; Law, M.; Tan, D. H.; Montano, M.; Goldberger, J.; Somorjai, G.; Yang, P. *Nano Lett.* **2005**, *5*, 1231.
(40) Greene, L. E.; Yuhas, B.; Law, M. *Inorg. Chem.* **2006**, *45*, 4977.
(41) Xu, S.; Wang, Z. L. *Nano Res.* **2011**, *4*, 1013.
(42) Baruah, S.; Dutta, J. *Sci. Technol. Adv. Mater.* **2009**, *10*, 013001.
(43) Vayssieres, L. *Adv. Mater.* **2003**, *15*, 464.
(44) Vayssieres, L.; Keis, K. *Chem. Mater.* **2001**, *13*, 52.
(45) Vayssieres, L.; Keis, K.; Lindquist, S.; Hagfeldt, A. *J. Phys. Chem. B* **2001**, *28*, 3350.
(46) Athauda, T. J.; Butt, U.; Ozer, R. R. *MRS Commun.* **2013**, *3*, 51.
(47) Baruah, S.; Thanachayanont, C.; Dutta, J. *Sci. Technol. Adv. Mater.* **2008**, *9*, 025009.
(48) Khan, A.; Abbasi, M. A.; Hussain, M.; Ibupoto, Z. H.; Wissting, J.; Nur, O.; Willander, M. *Appl. Phys. Lett.* **2012**, *101*, 193506.
(49) Ko, Y. H.; Kim, M. S.; Park, W.; Yu, J. S. *Nanoscale Res. Lett.* **2013**, *8*, 28.
(50) Manekkathodi, A.; Lu, M. *Adv. Mater.* **2010**, *22*, 4059.
(51) Goncalves, G.; Marques, P.; Neto, C. P.; Trindade, T.; Peres, M.; Monteiro, T. *Cryst. Growth Des.* **2008**, *9*, 386.
(52) Baruah, S.; Jaisai, M.; Imani, R.; Nazhad, M. M. *Sci. Technol. Adv. Mater.* **2010**, *11*, 055002.
(53) Kim, M. K.; Yi, D. K.; Paik, U. *Langmuir* **2010**, *26*, 7552.
(54) Guo, M.; Diao, P.; Cai, S. *J. Solid State Chem.* **2005**, *178*, 1864.
(55) Cheng, B.; Samulski, E. T. *Chem. Commun.* **2004**, 986.
(56) Xue, C.; Wang, R.; Zhang, J.; Jia, S.; Tian, L. *Mater. Lett.* **2010**, *64*, 327.
(57) Lee, Y. J.; Sounart, T. L.; Scrymgeour, D. A.; Voigt, J. A.; Hsu, J. W. P. *J. Cryst. Growth* **2007**, *304*, 80.
(58) Botelho, E. C.; Nogueira, C. L.; Rezende, M. C. *J. Appl. Polym. Sci.* **2002**, *86*, 3114.
(59) Djurisić, A. B.; Leung, Y. H. *Small* **2006**, *2*, 944.